

Low-frequency light scattering and structural defects in samarium phosphate glasses

G. Carini and M. Federico

Dipartimento di Fisica, Università di Messina, Contrada Papardo Salita Sperone, 31, 98010 S. Agata, Messina, Italy

A. Fontana

Dipartimento di Fisica, Università di Trento, 38050 Povo, Trento, Italy

G. A. Saunders

School of Physics, University of Bath, United Kingdom

(Received 3 August 1992)

Low-frequency Raman-scattering measurements have been made on samarium phosphate glasses containing 5 and 25 mol % Sm_2O_3 from 8 K to room temperature. The scattering due to acoustic modes has been separated quantitatively from the light-scattering excess (LSE). It has been shown that at low frequency the product $C(\omega)g(\omega)$ of the coupling constant $C(\omega)$ and density of states $g(\omega)$ has an ω^4 behavior, in good agreement with the predictions of the theoretical models for describing Raman scattering in a disordered system. The LSE is Lorentzian in form and its intensity increases with rising temperature in these glasses. Quantitative comparisons have been made between the behavior of the Raman scattering and the ultrasonic behavior determined in the same glass specimens. The magnitude of the LSE decreases with increasing samarium oxide content, while an opposite trend has been observed for the ultrasonic attenuation. This finding indicates that models that presuppose the structural relaxation of intrinsic defects in a glass as a common origin for the LSE and the low-temperature acoustic-loss peaks fail. It is suggested that the LSE and acoustic relaxations may result from different microscopic motions.

INTRODUCTION

It is well known that the supplementary degrees of freedom, which are frozen in a glass when the glass transition region is crossed, produce anomalies in a wide range of physical properties. These anomalies are usually attributed to microscopic units (single atoms and/or group of atoms), which are characterized by a different dynamics compared with those of the rest of the matrix. In the classification of Buchenau *et al.*,¹ the resultant low-energy excitations can be divided into three different groups as a consequence of the effects revealed in different intervals of temperature and frequency by thermal,² acoustic,³ Raman,^{4,5} and inelastic-neutron-scattering⁶ measurements. In particular, one type of additional excitation, arising from thermally activated motions of relaxing "particles" over potential barriers, is thought to cause the acoustic attenuation peak in the temperature region above 20 K, the excess of quasielastic contribution in the Raman,⁷ and inelastic neutron scattering (below 500 GHz). Attempts at revealing the detailed link between acoustic, optical, and neutron-scattering effects have been made in vitreous silica, one of the most studied glasses because pure single-phase specimens of suitable size are readily available. An acceptable interpretation of the relaxation effects in fused silica has been given in terms of two different models, one based on a distribution of "symmetric"⁶ and the other of "asymmetric"¹ double-well potentials, the latter emerging as the more convincing.

In addition to the light-scattering excess, another spectral component, the "boson peak," is usually observed at

a frequency shift of about 30 cm^{-1} . This feature has been explained in terms of light scattering from Debye-like acoustic modes associated with disorder.⁸⁻¹⁰ The most satisfactory model, that developed by Martin and Brenig¹⁰ has been used successfully to describe the Raman scattering in chalcogenide semiconducting¹¹ and some superionic glasses.¹² The main result obtained from this model is that a medium-range structural order exists with a structural correlation range of about 6–8 Å in those glasses.

The aim of this study has been to find out whether these models can explain quantitatively the dynamics of the low-frequency excitations in a wider class of amorphous systems. Raman-scattering measurements have been performed on glasses of the $\text{Sm}_2\text{O}_3\text{-P}_2\text{O}_5$ system and the results compared with those obtained of ultrasonic experiments.¹³ Analysis of the acoustic data pointed to the existence of a population of relaxing particles, whose concentration decreases as a function of the network modifier oxide (a common feature for all the phosphate glassy systems investigated up until now).^{13,14} The concentration decrease of the structural defects is used as a probe to ascertain the predictions of the model, which describes the light-scattering excess in terms of relaxing states. The structural correlation length, determined using the Martin and Brenig model¹⁰ for two different compositions, is discussed in the light of the structural information of these glasses.

EXPERIMENTAL RESULTS

The preparation and the characterization of the samarium phosphate glasses of composition

$(\text{Sm}_2\text{O}_3)_x(\text{P}_2\text{O}_5)_{1-x}$, x being the molar fraction, has been described elsewhere.¹⁶ It was not possible to make glasses from starting products containing more than 0.25 Sm_2O_3 because the melts were too viscous at the highest temperature (1800 K), which could be reached in the furnace. The samples were disc shaped, clear, pale yellow, and good optical quality glasses. This last property is very important, since it is essential to minimize the spectral component due the elastically scattered light, which could mask the very-low-frequency scattering.

The Raman-scattering experiments were carried out with a standard system in HV (depolarized) and VV (polarized) configurations. To avoid undue heating of the sample, the 5145-Å argon-laser line was used at a nominal power level, which was always below 80 mW. The spectral bandpass was 2.0 cm^{-1} .

EXPERIMENTAL RESULTS

The Raman spectra were measured on glasses with two quite different compositions (5 and 25 mol % Sm_2O_3) from liquid helium to room temperature. The resultant Raman spectrum can be divided in two frequency regions: high frequency (above 300 cm^{-1}) and the low-frequency part. The high-frequency spectral features were found to coincide with those previously obtained,¹⁶ so that attention will be focused on the low-frequency region. In the frequency region between 300 and 400 cm^{-1} the same shape characterized the spectra of each glass examined so that it was possible to use this part of the spectrum to normalize the data. The normalized Raman spectra of the two glasses at room temperature are shown in Fig. 1. It is clear that the boson peak is more intense for the glass with $x=0.25$ than for the sample with $x=0.05$.

Another scattering process is present: the so-called light-scattering excess (in the following denoted LSE), which is not seen in the crystalline state. Such scattering increases with rising temperature, more rapidly than that predicted by the Bose-Einstein population factor (Fig. 2). To examine the LSE quantitatively, it is necessary to

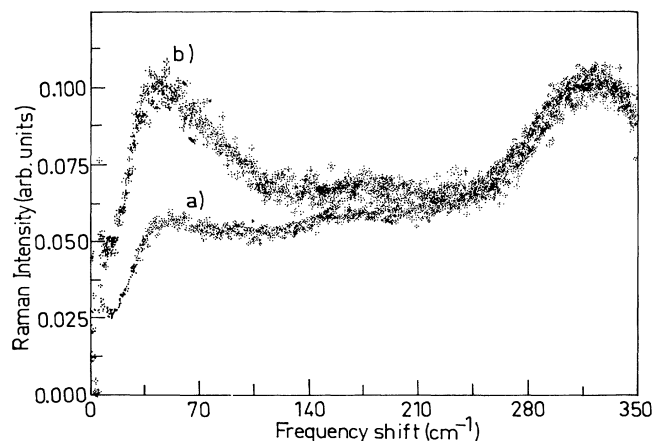


FIG. 1. Experimental Raman scattering at room temperature on samarium phosphate glasses with two molar fractions of Sm_2O_3 : (a) $x=0.05$ and (b) $x=0.25$.

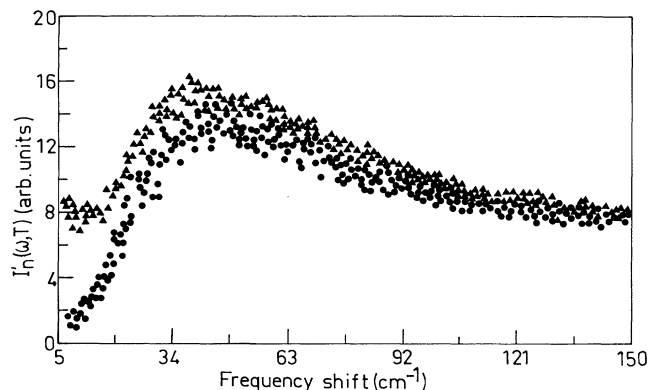


FIG. 2. $I/\omega[n(\omega, T)+1]$, denoted as I'_n , for $(\text{Sm}_2\text{O}_3)_x(\text{P}_2\text{O}_5)_{1-x}$ glasses of composition $x=0.25$; 15 K (filled circles) and 300 K (triangles). The intensity has been divided by ω in order to display the LSE.

evaluate the contribution in the low-frequency range of the scattering due to acoustic modes.

The Raman intensity in an amorphous system is given by

$$I(\Omega_0, \omega) = \frac{(\Omega_0 + \omega)^4}{2\pi c^3} \hbar V E_0^2 \sum_b c_b(\Omega_0, \omega) g_b(\omega) \frac{n(\omega, T) + 1}{\omega} \quad (1)$$

in the notation of the Galeener and Sen.⁹ This refers to a Stokes process, where Ω_0 is the frequency of the incident light, ω is the Raman shift, E_0 is the incident electric field amplitude, V is the scattering volume, b distinguishes acoustic and optic bands, and $g_b(\omega)$ is the corresponding density of states; $n(\omega, T)+1$ is the Bose-Einstein population factor, and $1/\omega$ is the harmonic propagator. The coupling constant $C_b(\omega)$ is given by

$$C_b(\omega) = \left[\sum_l P^2 u_l(\omega) \right]^2, \quad (2)$$

where only first-order terms of the expansion of the electronic polarizability as a function of the displacement eigenvector $u_l(\omega)$ have been retained. In the acoustic region it can be assumed that

$$C_b(\omega) = C_{ac}(\omega) \equiv C(\omega) \quad (3)$$

and

$$g_b(\omega) = g_{ac}(\omega) \equiv g(\omega). \quad (4)$$

Thus the Raman spectra of a disordered material, when reduced by the harmonic propagator and the population factor, reflects the density of states modulated by the coupling constant:

$$\frac{I^{\text{exp}} \omega}{n(\omega, T) + 1} \equiv I_R = C(\omega) g(\omega), \quad (5)$$

where I_R is the reduced intensity. In the low-frequency region, where the vibrational modes are acoustic, the density of states is expected to be Debye-like and hence to have an ω^2 behavior. Thus, in this frequency range,

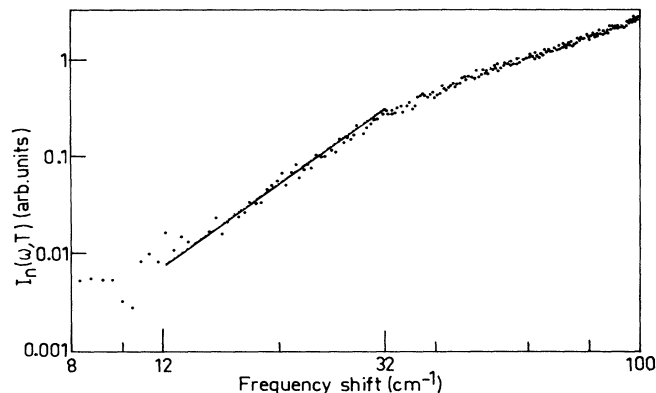


FIG. 3. Log-log plot of reduced Raman intensity $I_n(\omega, T)/[n(\omega, T)+1]$, denoted as $I_n(\omega, T)$, for samarium phosphate glass of composition $x=0.05$ at 8 K. The slope of the straight line is 3.8.

the coupling constant for light scattering from acoustic modes may be determined from Raman measurements.

To nullify any disturbance from the LSE, it is expedient to consider the Raman spectrum at liquid-helium temperature, where its effects are negligible. A log-log plot of the reduced intensity against frequency shift (Fig. 3) evidences a frequency region in which the slope is close to 4. An ω^2 dependence of $C(\omega)$ is obtained from Eq. (5) if the density of states $g(\omega)$ is proportional to ω^2 , in agreement with theoretical models developed to explain the Raman scattering in amorphous systems (reviewed in Ref. 6). Hence, this result gives confidence that the scattered intensity at low temperatures is due only to acoustic modes.

Now it is possible to determine the LSE. Figure 4 shows, as a typical example, the ratio between reduced spectra taken at 8 and 300 K (the latter being the highest temperature at which measurements have been made) for a sample with a composition of x of 0.25. It is evident from this figure that beyond about 50 cm^{-1} the Raman intensity exhibits a temperature dependence proportional to $n(\omega, T)+1$; so it is straightforward to normalize the

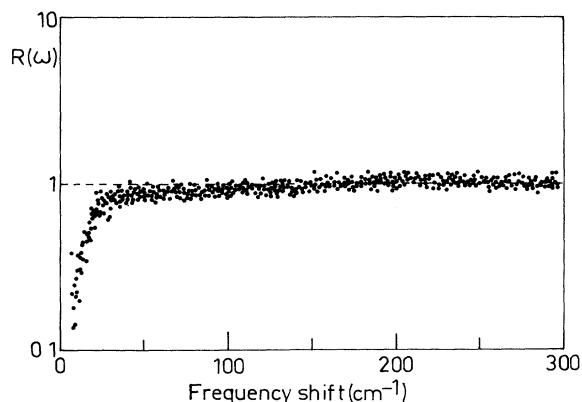


FIG. 4. Ratio $R(\omega)$ between the normalized Raman spectra at 8 and 300 K in the samarium phosphate glass of composition $x=0.25$ (see text).

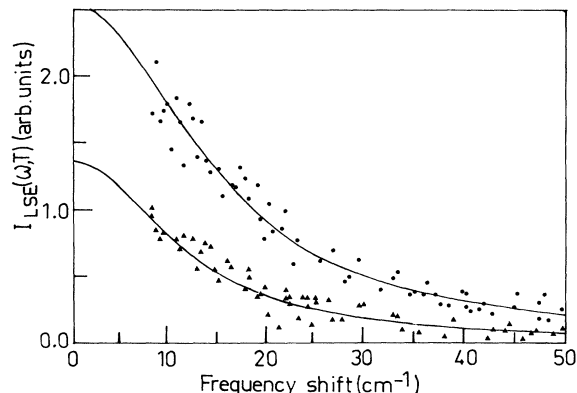


FIG. 5. Room-temperature light-scattering excess as derived from Eq. (6) for the samarium phosphate glasses with compositions $x=0.05$ (triangles) and $x=0.25$ (filled circles).

reduced spectra, measured at several temperatures, in the frequency range above 50 cm^{-1} . The reduced spectrum obtained at the lowest temperature (8 K) has been subtracted from those at higher temperatures, and the results multiplied by $n(\omega, T)+1$. Therefore, the LSE spectra at a given temperature can be expressed as

$$I^{\text{LSE}}(\omega, T) = \frac{I^{\text{LSE}}(\omega, T)}{n(\omega, T)+1} - a \frac{I^{\text{exp}}(\omega, 8 \text{ K})}{n(\omega, 8 \text{ K})+1} [n(\omega, T)+1], \quad (6)$$

where a is the normalization factor in the frequency range above 50 cm^{-1} .

The results obtained for 5 and 25 mol % Sm_2O_3 phosphate glasses are shown in Fig. 5. Complete data are collected in Table I.

A major feature is that the LSE has a Lorentzian spectral shape (within the limits of experimental error) in-

TABLE I. Parameters derived from experimental light-scattering data for samarium phosphate glasses. The intensity of light-scattering excess I^{LSE} has been obtained as the area of the Lorentzian fit, W is the width at half height, and I^{10} is the intensity at 10 cm^{-1} .

x	T (K)	I^{LSE} (arb. units)	ω (cm^{-1})	I^{10} (arb. units)
0.05	47			
	85	81	8.1	3.9
	110	100	9.1	5.0
	160	166	8.6	8.4
	250	377	9.2	18.8
	293	496	10	24.7
0.25	45	28	16	1.3
	80	88	15.7	4
	110	206	16.7	8.6
	150	314	16.5	14
	200	400	14	19
	250	570	15	26
	300	782	15.1	36

dependent of temperature for all the samples, although the widths may differ. In addition, the integrated intensity increases differently with temperature in the two glasses. It is difficult to obtain the precise law with which the intensity increases because of the limits imposed by the available temperature range; an extension of the experiment above room temperature should provide more insight.

DISCUSSION

Scattering from acoustic modes

The low-frequency region of the Raman spectra in both the glasses studied is typical of the "glassy state." An intense low-frequency band at about 35 cm^{-1} is present in all the amorphous systems investigated up till now^{5,11,12} and can be considered an indicator of the structural disorder characterizing a glassy network. Martin and Brenig¹⁰ have suggested that the lack of periodicity in the structure induces electrical and mechanical disorder, giving rise to spatial fluctuations in the photoelastic and elastic constants.

Interesting consequences of the model are the representation of the spatial fluctuations in the Raman coupling constants by a structural correlation range (SCR) and the direct relation between the maximum frequency of the peak ω_{max} and the SCR.¹¹ By weighting the fluctuations in the elastic and photoelastic constants by Gaussian functions, the Raman coupling constants can be expressed by the following formula:

$$C_{HV}(\omega) = A \omega^2 \left\{ \left[3 \left(\frac{v_l}{v_t} \right)^5 \exp \left[- \frac{(2\pi c \omega)^2 \sigma^2}{v_t^2} \right] \right] + 2 \exp \left[- \frac{(2\pi c \omega)^2 \sigma^2}{v_l^2} \right] \right\} \quad (7)$$

with $\sigma = \bar{v} / 2\pi c \omega_{\text{max}}$, where $C_{HV}(\omega)$ is the depolarized component of the coupling function, v_l and v_t are the longitudinal and transverse sound velocity, \bar{v} the average sound velocity, and 2σ is the structural correlation length. The sound velocities have been measured in the ultrasonic range by a pulse-echo technique.¹³

This expression leads to an ω^2 dependence for $C(\omega)$, in the low-frequency limit, in agreement with the experimental results reported here. Typical best fits of experimental data normalized by the factor $\omega[n(\omega, T) + 1]$ are reported in Fig. 6 for both the glass compositions. The agreement between the theoretical curve and the experimental points below 60 cm^{-1} supports the theoretical approach. The values of the SCR, obtained from the fits, change slightly with samarium oxide content, being 5.7 \AA for $x=0.05$ and 6.2 \AA for $x=0.25$; this magnitude is similar to that obtained in chalcogenide glasses.¹¹ It can be concluded that the samarium concentration up to $x=0.25$ does not appreciably modify the local order characterizing the phosphate glass as far as the mechanical and the electrical disorder is concerned. There is an interesting, and instructive, possible association of the SCR with a characteristic length in the phosphate net-

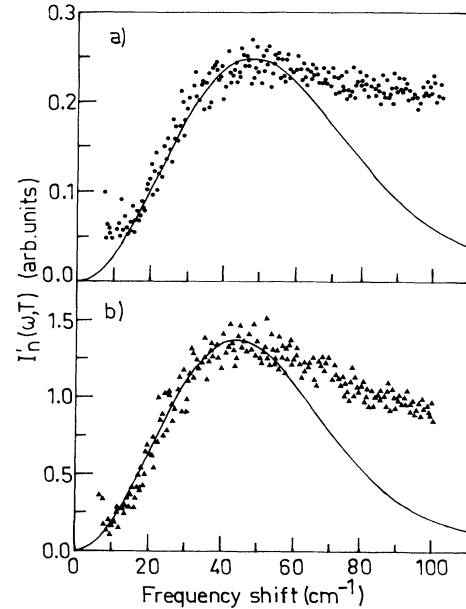


FIG. 6. The experimental Raman scattering data divided by the frequency and the population factor in the samarium phosphate glasses of compositions (a) $x=0.05$ and (b) $x=0.25$ samples. Solid lines are the fits obtained from the Martin-Brenig model. The fit parameters are in Table II.

work. Phosphate glass structures are based on interconnecting phosphorus-oxygen tetrahedral units with a diameter slightly more than 3 \AA .¹⁵ However, on the basis of theoretical arguments used to describe the elastic behavior of vitreous oxides, it has been suggested that the structure of vitreous P_2O_5 may be built from three dimensionally connected P_6O_6 rings.¹⁵ The average diameter of such a ring is approximately 6 \AA , in agreement with the SCR values obtained in samarium phosphate glasses, indicating that the ringlike structures rather than the tetrahedral units contribute strongly to the low-frequency vibrational spectrum of this kind of glass.

Light-scattering excess

Jackle⁶ proposed a model that attributed the LSE to the structural relaxation of a population of defects with different polarizability, represented in terms of symmetric double-well potentials. In the framework of this model the microscopic origin of the LSE should be the same as that which causes the acoustic-loss peaks revealed for temperatures above 20 K in a wide range of glasses.^{13,14,16,18} Since the acoustic loss is usually analyzed in terms of a Gaussian distribution of relaxation

TABLE II. Transverse v_t , longitudinal v_l , and average \bar{v} ultrasound velocities and the structural correlation length σ for samarium phosphate glasses.

x	v_t (10^5 cm/s)	v_l	\bar{v}	2σ (\AA)
0.05	2.825	4.755	3.127	5.7
0.25	2.522	4.422	2.797	6.2

times, due to random deviations in the local arrangement of the loss centers (the relaxing particles), the excess of scattering can be written as⁶

$$I_{HV}(\omega) \propto \frac{n(\omega, T) + 1}{4K_B T} \int dE P(E) \frac{\tau(E)}{1 + \omega^2 \tau^2(E)}. \quad (8)$$

where

$$P(E) = \frac{1}{\sqrt{2\pi}E_0} \exp \left[-\frac{(E - E_m)^2}{2E_0^2} \right]$$

and

$$\tau(E) = \tau_0 \exp \left[\frac{E}{K_B T} \right].$$

Here $P(E)$ is the distribution of the activation energies, and $\tau(E)$ is the temperature activated relaxation time. In the case where a single value for the characteristic time τ_0 is assumed, the τ distribution corresponds to a distribution of the activation energies E for the barrier height between the two wells.

Subsequently Gilroy and Phillips⁹ criticized the "symmetric-well" approach and proposed a model based on "asymmetric-double-well potential" having a distribution of both the relaxation time and the asymmetry $f(\Delta, \tau)$. In this case the intensity of the light scattering excess is given by

$$I_{HV}(\omega) \propto \frac{n(\omega, T) + 1}{4K_B T} \int \int d\Delta d\tau f(\Delta, \tau) \frac{\tau}{1 + \omega^2 \tau^2} \times \text{sech}^2 \frac{\Delta}{2K_B T}, \quad (9)$$

where

$$\tau = \tau_0 \exp(E/K_B T) \text{sech}(\Delta/2K_B T).$$

Application of these models provided a successful interpretation for the scattering data in vitreous silica; in particular, the "asymmetric-well model" permitted a unified and more refined description of the acoustic, optic, and quasielastic neutron-scattering measurements. Nevertheless it should be emphasized that this model was unable to describe quantitatively the ultrasonic relaxation loss observed in vitreous silica in the "MHz" region, when the same parameters required to fit the experimental attenuation at 660 KHz were used.¹⁹

Inserting in Eq. (8) the parameters derived from an ultrasonic study in the same samples of the phosphate glasses¹³ gives the curves shown in Fig. 7, which includes the experimental data of LSE obtained by the procedure described above. The frequency used was 10 cm^{-1} for both experimental and theoretical data (the temperature behavior at different frequency shifts showed the same shape). Even when the theoretical and experimental data lie within a comparable intensity range, the following differences are evident from this comparison.

(1) The observed temperature behavior is very different from that predicted theoretically.

(2) The magnitude of the scattering excess is higher in the sample with $x = 0.25$ than in that with $x = 0.05$ over the whole temperature range, while the opposite trend is

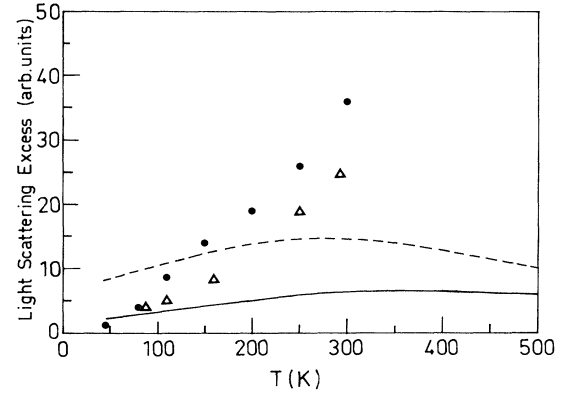


FIG. 7. Experimental light-scattering excess at 10 cm^{-1} vs temperature in the samarium phosphate glasses of compositions $x = 0.05$ (triangles) and $x = 0.25$ (filled circles). The curves shown as dotted ($x = 0.05$) and solid ($x = 0.25$) lines, have been derived by using Eq. (8) and the same parameters obtained by the fit of ultrasonic data.

predicted from ultrasonic results (shown by the curves in Fig. 7).

To attempt a comparison of the LSE with the behavior predicted by Eq. (9) for the asymmetric-well model, a fit of the ultrasonic attenuation data was carried out by considering that $f(\Delta, \tau)$ arises from distributions of both asymmetries $g(\Delta)$ and a barrier energy $P(E)$. When $g(\Delta)$ was taken as being constant up to a maximum value of $\Delta \approx 2kT$ and $P(E)$ chosen as having either a Gaussian or exponential distribution, the agreement between the theoretical and the experimental data was found to be inferior to that obtained by the symmetric-well model, particularly when the exponential barrier distribution was used. This circumstance precluded any further attempts at a comparison of the LSE with the behavior expected by the asymmetric-well model. The study indicates that neither of the models proposed to explain the structural relaxation in vitreous silica adequately describes the present results for samarium phosphate glasses, the situation found previously for chalcogenide¹¹ and silver phosphate²⁰ glasses. Different microscopic motions need to be taken into consideration to account for the anomalies revealed by the acoustic probe and the light scattering.

The increase of LSE with the samarium content can be qualitatively understood from structural considerations. It has been inferred¹⁷ that during the glass formation the addition of a metal oxide to P_2O_5 results in reduction of the number of cross-linking P—O—P bonds between pairs of tetrahedra: the system tends to form chains of PO_4 tetrahedra, which are connected at two corners and have two nonbridging oxygen atoms. As a consequence we can distinguish between "constrained" PO_4 tetrahedra, some groups with three bridging oxygens and the fourth doubly bonded, and other "underconstrained" PO_4 tetrahedra, having more nonbridging oxygens. Then the SLE could be interpreted as arising from the local motions of the underconstrained PO_4 units, which can reorientate more easily than the rest of the system and are formed in increasing numbers when Sm_2O_3 is added to P_2O_5 .

CONCLUSIONS

(1) Light-scattering measurements on samarium phosphate glasses have established the presence of an excess of light scattering, which is superimposed on the low-frequency part of the disorder-induced one-phonon scattering. It has proved possible to resolve these two contributions and to verify that the low-frequency scattering behaves approximately as ω^4 .

(2) By applying the Martin and Brenig model¹⁰ a structural correlation length of about 6 Å has been found, which seems to connect the low-frequency scattering to ringlike structures that exist in this kind of glass.

(3) The intensity of the LSE has been found to be strongly temperature dependent, while its shape is invari-

ant for all the measured temperatures.

(4) Finally it has been shown that the Jackle-Phillips models are not able to account fully for the experimental data. Most importantly the LSE and the acoustic relaxation losses do not have the same microscopic origin. The magnitude of LSE is increased by increasing the Sm₂O₃ content, this being an opposite tendency to that shown by the ultrasonic relaxation loss. The behavior observed suggests that the LSE is associated with particles, which should be characterized by a higher polarizability than the rest of the system, namely, the PO₄ tetrahedra with two nonbridging oxygens. To obtain more insight into the microscopic mechanisms, which are responsible for this spectral component, revision of the existing models is needed.

¹U. Buchenau, H. M. Zhou, N. Nucker, K. S. Gilroy, and W. A. Phillips, *Phys. Rev. Lett.* **60**, 1318 (1988).

²R. O. Pohl, in *Amorphous Solids*, Topics in Current Physics Vol. 24, edited by W. A. Phillips (Springer-Verlag, Berlin, 1981), p. 27.

³S. Huklinger and M. V. Schickfus, in *Amorphous Solids* (Ref. 2), p. 81.

⁴G. Winterling, *Phys. Rev. B* **12**, 2432 (1975).

⁵A. Fontana, G. Mariotto, and F. Rocca, *Phys. Status Solidi B* **129**, 489 (1985); A. Fontana and F. Rocca, *Phys. Rev. B* **36**, 9279 (1987).

⁶J. Jackle, in *Amorphous Solids* (Ref. 2), p. 135.

⁷U. Buchenau, M. Prager, N. Nucker, A. J. Dianoux, N. Ahmad, and W. A. Phillips, *Phys. Rev. B* **34**, 5665 (1986).

⁸R. Shuker and R. W. Gammon, *Phys. Rev. Lett.* **25**, 222 (1970).

⁹F. L. Galeener and P. N. Sen, *Phys. Rev. B* **17**, 1928 (1978).

¹⁰A. Martin and W. Brenig, *Phys. Status Solidi B* **64**, 163 (1974).

¹¹R. J. Nemanich, *Phys. Rev. B* **16**, 1655 (1977).

¹²G. Carini, M. Cutroni, A. Fontana, G. Mariotto, and F. Rocca, *Phys. Rev. B* **29**, 3567 (1984).

¹³G. Carini, M. Cutroni, G. D'Angelo, M. Federico, G. Galli, G. Tripodo, G. A. Saunders, and W. Qingxian, *J. Non-Cryst. Solids* **121**, 288 (1990).

¹⁴B. Bridge and N. D. Patel, *J. Mater. Sci.* **21**, 3783 (1986).

¹⁵B. Bridge, N. D. Patel, and D. N. Waters, *Phys. Status Solidi* **77**, 655 (1983).

¹⁶G. Carini, M. Cutroni, M. Federico, and G. Galli, *J. Non-Cryst. Solids* **104**, 323 (1984).

¹⁷A. Mierzejewski, G. A. Saunders, H. A. A. Sidek, and B. Bridge, *J. Non-Cryst. Solids* **104**, 323 (1988).

¹⁸R. E. Strakna and H. T. Savage, *J. Appl. Phys.* **35**, 1445 (1964).

¹⁹K. S. Gilroy and W. A. Phillips, *Philos. Mag.* **43**, 735 (1981).

²⁰P. Benassi, A. Fontana, and P. A. M. Rodrigues, *Philos. Mag.* **65**, 173 (1992).